ELSEVIER

Journal of Chromatography A, 741 (1996) 151–163

JOURNAL OF CHROMATOGRAPHY A

Mathematical modelling and computer simulation of aqueous two-phase continuous protein extraction[1]

S.L. Mistry[a], A. Kaul[a], J.C. Merchuk[b], J.A. Asenjo[c,*]

[a]*Biochemical Engineering Laboratory, The University of Reading, Reading, UK*

[b]*Department of Chemical Engineering, Ben Gurion University, Beer Sheva, Israel*

[c]*Centre for Biochemical Engineering and Biotechnology, University of Chile, Beauchef 861, Santiago, Chile*

Received 8 September 1995; revised 21 February 1996; accepted 4 March 1996

Abstract

An extended mathematical model has been developed to describe the continuous, steady state operation of an aqueous two-phase system for protein extraction. The basic model is based on steady state mass balances of the main components and phase equilibrium data. Phase equilibrium (binodial curve) was fitted by an equation that relates poly(ethylene glycol) (PEG) to phase forming salt (e.g phosphate) and added NaCl. Experimental data on the separation of α-amylase from *B. subtilis* supernatant in a PEG4000/phosphate system was used. The data show the effect of NaCl which was used to carry out the extraction of α-amylase into the PEG phase and back into the salt phase. The partition coefficient of the α-amylase was fitted to a sigmoidal Boltzman curve and gave a very good fit. Two simulations were carried out to show the effect of phase ratio on purification and this was represented in an equilibrium system diagram of material balances. The model has been extended to account for phase separation kinetics and thus aspects of continuous processing. Modelling the rate of settling of the two phases using appropriate correlations has been presented and discussed.

Keywords: Continuous protein extraction; Aqueous two-phase systems; Computer simulation; Mathematical modelling; Material balance diagram; Phase separation kinetics; Proteins; α-Amylase

1. Introduction

Aqueous two-phase systems (ATPS) exploit the incompatibility between aqueous solutions forming two phases [1]. They can be used to separate therapeutic and other proteins from contaminants and therefore represent an inexpensive and effective initial downstream processing step [2,3]. These systems can be relatively sensitive to their environmental conditions and hence, a mathematical model can be useful to describe the effect of key parameters on performance to assist in process design and scale up, to perform simulations for process optimisation and to find robust process conditions. Experimental data on phase equilibrium is available and this can be used as a base for modelling. Engineering models for equilibrium phase formation in ATPS have only started to be reported in the literature. Models for phase separation are also scarce.

ATPS are usually composed of aqueous solutions of polyethylene glycol (PEG) and salt (e.g. phos-

* Corresponding author. Present address: The Sanger Centre, Hinxton Hall, Hinxton, Cambridge CB10 1RQ, UK.

[1] Presented at the 9th International Conference on Partitioning in Aqueous Two-Phase Systems, Zaragoza, June 4–9, 1995.

0021-9673/96/$15.00
PII S0021-9673(96)00179-3

phate or sulphate) or PEG and dextran. The former system is more commonly used [2,4–6]. Differences in the relative partitioning of the proteins and cell debris between the two phases will result in the constituents partitioning independently. Most soluble and particulate matter will partition to the lower, more polar phase of phosphate salt and when the system properties have been properly manipulated (e.g. addition of NaCl), the product protein will partition to the top less polar phase, consisting of PEG. This has been successfully carried out for a number of proteins like thaumatin [4], tPA [5] and α-amylase [6].

Schmidt et al. [6] show the effect of NaCl concentration on the partition coefficients (K) for α-amylase and *B. subtilis* contaminants in PEG/phosphate and PEG/sulphate systems. The K of α-amylase at the low NaCl concentration was several folds smaller than that of the contaminants. At the high NaCl concentrations, the K of α-amylase in this system is several folds greater than that of the contaminants. This feature can be exploited for extracting a particular protein from its contaminants in a first extraction, in the presence of high concentration of NaCl, and then back-extracting the protein in a second salt phase (phosphate or sulphate) without NaCl. The NaCl still present in the PEG phase (from the first extraction) is now diluted into the (sometimes larger) bottom phase thus dramatically lowering the partition coefficient of the product protein and allowing its back-extraction into the salt phase.

A very simple mathematical model was previously proposed to describe the continuous steady state operation of an aqueous two-phase system for protein extraction [7] using experimental data on the separation of thaumatin from contaminant proteins of an homogenate of *E. coli* [4]. In that simple model however, partition coefficients were taken as constant and for the binodial, an exponential curve that did not give a very good fit was used. Recently it has been shown that a polynomial will fit the binodial better [8].

The aim of this paper is to develop a realistic mathematical model that will take into account the effect of added NaCl on the partition coefficients of the target protein and the protein contaminants as this is a key process feature and will also include the effect of added NaCl on the displacement of the binodial curve. The extension of the model to include the kinetics of phase separation is presented and discussed.

2. Materials and methods

2.1. Materials

PEG with M_w 4000 was obtained from Fluka Chemicals, Buchs, Switzerland. All other chemicals were analytical grade.

2.2. Partitioning of α-amylase

Partitioning experiments of α-amylase and its contaminants were carried out using an industrial crude supernatant of *B. subtilis* kindly donated by Rhône-Poulenc, ABM Brewing and Food Group, Stockport, Cheshire, UK, as previously described [6].

2.3. Preparation of phase systems

Phase systems were prepared from stock solutions of PEG (50% w/w), phosphate (40% w/w) and NaCl (25% w/w). The phosphate stock solution consisted of a mixture of K_2HPO_4 and NaH_2PO_4 at the appropriate pH. Stock solutions were stored at 4°C and were temperature equilibrated before use by standing at room temperature (20°C). The phase volume ratios were determined in graduated centrifuge tubes.

2.4. Batch separation of phase systems

For all the experiments, the time for complete phase separation was defined as the time required for the main bulk of the phases to separate and a horizontal interface to be formed. However very small drops of one phase remain in the other for a period of time even after a horizontal interface is formed.

2.4.1. Small scale

Separation studies were carried out in 10-ml graduated centrifuge tubes for pure systems. Systems were mixed for 2 min using a vortex-mixer to ensure

complete mixing. The height of the dispersion was measured as a function of time. Triplicate readings were taken. The accuracy of the measurements was well within ±5% of the reading.

2.4.2. Large scale

Separation studies were carried out in a Bioengineering 2-l impeller agitated reactor with a height to diameter ratio of 1.83. The height of the dispersion was measured as a function of time. Triplicate readings were taken.

2.5. Identification of the continuous phase: effect of volume ratio

For studies on the effect of volume ratio on phase separation time, nine 150-g PEG–phosphate systems were prepared from stock solutions. After phase separation, the top and bottom phases of the systems were separated and used as stocks for the preparation of further systems. To make systems with different volume ratios, certain amounts of top and bottom phase stocks were mixed in 10-ml graduated cylinders. The time for complete separation, after vigorously shaking the of graduated cylinders for 30 s to ensure complete mixing, was noted. Care was taken to ensure that each system was mixed in the same manner. Detection of the continuous phase was carried out by visual observation and is discussed in more detail later on.

3. Model development

3.1. Phase diagrams

The effect of concentration of the phase constituents on a phase diagram (Fig. 1) show the state of the system with its characteristic binodial curve (TCB). All points in the homogeneous region (to the left of TCB) will only form one phase, while any mixture in the heterogeneous region (to the right of TCB) will separate into two phases.

The point M therefore represents a two-phase system consisting of a top phase of composition T and a bottom phase of composition B. Tie lines connect phase compositions on TCB which are in equilibrium with each other. Where the tie line cuts the binodial represents the top and bottom phases that will form. Points on the same tie line give rise to systems with identical top and bottom phase compositions but with differing mass of phases. The phase mass ratio is given by (inverse lever rule):

$$\frac{V_T \rho_T}{V_B \rho_B} = \frac{MB}{MT} \quad (1)$$

where V and ρ are the volume and density of the phases, respectively.

The critical point, C, represents the point where the compositions and volumes of the two phases are equal.

The partition coefficient, K, describes the protein distribution between the phases and is defined as:

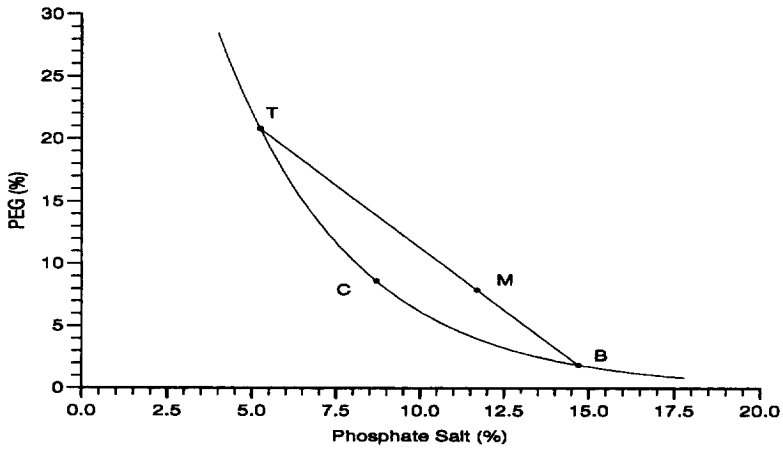

Fig. 1. Typical phase diagram.

$$K = \frac{C_T}{C_B} \quad (2)$$

where C_T = concentration in top phase and C_B = concentration in bottom phase.

For good separation and purification, the product should have a high partition coefficient and the contaminants should have a very low partition coefficient. To optimise conditions for separation, the partition coefficient can be manipulated by altering specific parameters such as molecular weight of polymer, type of ions included in the system, the ionic strength, or the use of modified polymers which have a higher affinity for the required protein.

3.2. Description of the process

The first stage in the flow scheme (Fig. 2) is the major separation step. Target and contaminant proteins enter the process via stream F_1, either in the form of whole or disrupted cells or just soluble proteins after cell debris removal. The recycle stream F_2 from Stage 2 consists of the top PEG phase after back extraction of the product protein into the salt phase. The high NaCl concentration aids the product protein partitioning to the top phase in Stage 1 while the partitioning of the contaminant [6] is unaffected and leaves via the bottom phase waste stream, F_3, with virtually no product. Stream F_4 passes on the product rich top phase to Stage 2 for back extraction. Fresh PEG and phosphate are continuously added in Stage 1 to account for phase component losses from the system.

Extra phosphate is added by stream F_5 to dilute the NaCl concentration. This aids product partitioning back into the lower phosphate phase. The top phase is then recycled to minimise PEG loss and also increase the process yield. F_6 is the final product output stream from the bottom phase of Stage 2. The mathematical model of the process is composed of mass balances and phase equilibrium relationships. These are described below.

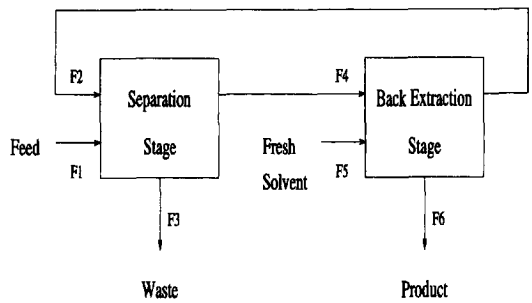

Fig. 2. Flow scheme of process.

3.3. Mass balances

The steady state mass balances account for the main components, i.e. flow-rates, phase forming chemicals and the proteins present in both stages.

$$\sum_{in} F_i = \sum_{out} F_i \quad (3)$$

$$\sum_{in} F_i P_i = \sum_{out} F_i P_i \quad (4)$$

$$\sum_{in} F_i X_i = \sum_{out} F_i X_i \quad (5)$$

where i = stream number, F = flow-rate ($m^3 s^{-1}$), P = phosphate, PEG or NaCl concentration (kg m^{-3}) and X = product or contaminant concentration (kg m^{-3}).

These equations are written for each stage j.

3.4. Phase equilibrium

The phase equilibrium for an aqueous two-phase system can be represented as a binodial curve relating the phosphate and PEG concentrations. The binodial is known to vary in the presence of NaCl, so this was modelled over the range of 0–10% NaCl. The binodial data for a PEG4000–phosphate system at pH 7 was collected and fitted to an equation of the form:

$$\ln(Y) = A + BX^3 + C\sqrt{X} \quad (6)$$

where Y = PEG concentration and X = phosphate concentration.

The fitting was performed using "Tablecurve", a program that automatically fits 2000 different expressions to a set of experimental data and classifies the resulting equations according to the R square. The form of the equations is, therefore, empirical. The constants A, B and C are functions of the NaCl concentration and are given by:

$$A = A_0 + A_1 N + A_2 \sqrt{N}$$

$$B = B_0 + B_1\sqrt{N}$$

$$C = C_0 + C_1 N + C_2 N\sqrt{N}$$

where N is the NaCl concentration.

The resulting equation for each stream becomes:

$$\text{PEG}_i = f(\text{Phosphate}_i, \text{NaCl}_i) \quad (7)$$

3.5. Equilibrium phase separation

To model phase separation requires calculating the average concentration of the total incoming phase components to give a point on the phase diagram. This point then has an associated tie line whose equation must be calculated. Finally the outgoing phase components are calculated by finding the intersections of the tie line with the binodial curve.

Each separation stage has two incoming streams and the average concentration of the phase components is given by the general formula:

$$\text{Average } P_{ij} = \left(\sum_{\text{in}} F_i P_i\right)\left(\sum_{\text{in}} F_i\right) \quad (8)$$

The tie line associated with this point has the equation of a straight line relating to the outgoing streams:

$$\text{PEG}_{ij} = D_{1j} \cdot \text{Phosphate}_{ij} + D_{2j} \quad (9)$$

where D_1 = gradient of line and D_2 = intercept of line.

Experiments were carried out to ascertain the effect of the salt concentration on the gradient, D_1, of the tie lines.

The value of D_2 is found by using the average concentration of the incoming phase components, which gives:

$$D_{2j} = (\text{Average PEG}_j) - D_{1j}(\text{Average Phosphate}_j) \quad (10)$$

Thus, the outgoing phase compositions can be calculated.

3.6. Partition coefficients

The equilibrium relationship for the concentration of proteins (K_p) and contaminants (K_c) in each phase can now be expressed as:

$$K_{p_j} = \frac{\text{Protein}_T}{\text{Protein}_B} \quad (11)$$

$$K_{c_j} = \frac{\text{Contaminant}_T}{\text{Contaminant}_B} \quad (12)$$

In a particular ATPS, the partition coefficient of a protein will be constant over a range of protein concentrations as long as the protein concentration is below its saturation range [1]. The partition coefficient of the contaminants should also be constant when operating in the linear range for the individual proteins even if it represents the value of K of a mixture of proteins. This is true as soluble protein composition of an homogenate of *Escherichia coli* or *B. subtilis* supernatant made under industrial conditions is relatively constant. The only other factor that could affect this behaviour would be if the added homogenate would significantly affect the phase composition of the phases thus maybe affecting the partition behaviour of the proteins.

A function relating the partition coefficient to the concentration of NaCl was fitted instead of using constant values of K, as used previously [7,8]. The partition behaviour of α-amylase [6] was studied to show the effect of the salt concentration on the partition coefficient (K_p). The partition behaviour of the protein as a function of NaCl concentration in the system was fitted to a sigmoidal Boltzman curve of the form:

$$\log K_p = \frac{G_1}{1 + \exp\left\{\dfrac{(\text{NaCl} - G_3)}{G_4}\right\}} + G_2 \quad (13)$$

Partitioning of contaminants [6] was much simpler and could be modelled by a straight line as they were not a strong function of the concentration of NaCl.

$$\log K_c = \text{E}_1\text{NaCl} + \text{E}_2 \quad (14)$$

3.7. Kinetics of phase separation

The steady-state model described above makes two important assumptions, (1) total equilibrium is obtained in each of the contacting stages, (2) complete separation of the two phases can be obtained after each mixing/equilibration stage.

These assumptions do not take into consideration

the performance of the equipment used for mixing and for separation. If the mixers and settlers used do not comply with the ideal behaviour assumed, deviations from the performance predicted by the model will occur. In this situation, the kinetics of mixing and phase separation will have to be considered. In aqueous two-phase systems, mixing is considered to be very rapid due to the low interfacial tension but phase separation kinetics can be critical [9].

4. Mixing

The principal issue here is that there is a minimum time required to complete mixing at the molecular scale (micromixing). It will be assumed that the time required for macromixing, t_m, can be taken instead [10]. In general, we will be able to find a function of the type:

$$(N \times t_m) = f_1(\text{Re, Impeller Type}) \tag{15}$$

where Re is the Reynolds number.

Efficient mixing requires turbulence and this establishes the lower limit for N. It has been reported [10] that under such conditions, the function f_1 becomes a constant, I:

$$t_m = \frac{I}{N} \tag{16}$$

where I depends only on the impeller type.

For a given total flow-rate, t_{mj} can be used to calculate the volume of the mixer, V_{mj} in each stage:

$$V_{mj} = J t_{mj} \sum_{in} F_{ij} \tag{17}$$

The constant J takes into account that the required time in the mixer which includes phase formation, is larger than the mixing time given by Eq. 16.

In the case of on line mixers, the requirements of a minimum N is replaced by the election of the diameter of the tube (which together with the total flow-rate establishes the Re). Once the diameter is fixed, a function relating t_m (or number of mixing elements) to flow-rate will give the minimal volume of mixer required.

4.1. Phase separation

The separation after complete formation of the equilibrated phases has been achieved is a time-dependent process. In general, the height changes as a function of time until the system is fully settled:

$$\left(\frac{dh}{dt}\right) = f_2(\Delta_\rho, \sigma, \mu_h, \mu_l, d_d) = f_2(\text{Re, We}) \tag{18}$$

where We is the Weber number, h = height of the interphase, $\Delta\rho$ = density difference between the phases, σ = surface tension between the phases, μ_h = viscosity of the heavy phase, μ_l = viscosity of the light phase and d_d = droplet diameter.

The mean droplet diameter is a function of the hydrodynamic conditions in the mixer. In a stirred mixer, it will be a function of Re, We and t_m:

$$d_d = f_3(\text{Re, We}, t_m) \tag{19}$$

where the velocity of the droplets could be taken as proportional to N.

Integration of Eq. (18) gives the profile of interphase height as a function of time and from it the time required for a complete separation, t_{sj}, can be estimated as:

$$t_{sj} = f_4(\text{Re, We}) \tag{20}$$

The volume of the separator required in each stage, V_{sj} can now be obtained from:

$$V_{sj} = t_{sj} \sum_{in} F_{ij} \tag{21}$$

Eq. (21) gives the maximal value of separator volume, when complete disappearance of the interphase is assumed.

5. Results and discussion

5.1. Binodial fitting

A close up of the fitted binodials with the experimental points is shown in Fig. 3. It can be seen that the empirical equation used gave an excellent fit to the data and can now be used to model the binodial over the continuous range of NaCl concentrations from 0–10%. Table 1 shows the values

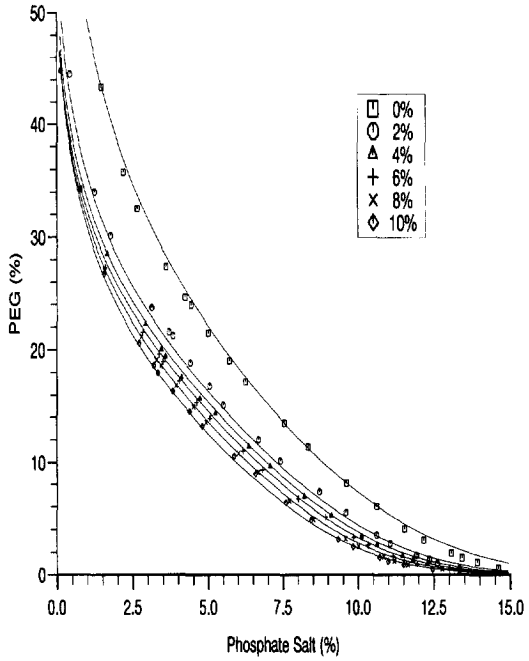

Fig. 3. Close-up of experimental points and fitted lines in center region.

of the constants obtained by fitting Eq. (6) to the experimental data obtained for each salt concentration.

5.2. Tie line variations

The tie line gradient for three different systems at various NaCl concentrations are shown in Table 2 and the actual tie lines with associated binodial are illustrated in Fig. 4. Considering that the relative variations were not statistically significant, it was decided to use $D_1 = -2.4$ throughout the rest of the model.

Table 1
Binodial function constants

A_0	4.472
A_1	0.06884
A_2	−0.3593
B_0	−0.0006540
B_1	−0.0001976
C_0	−0.5787
C_1	0.04224
C_2	−0.01395

Table 2
Tie line gradients at varying NaCl concentrations and at system compositions of (1) 12.5% phosphate, 10.7%o PEG, (2) 11.692% phosphate, 10.008% PEG and (3) 10.666% phosphate, 9.13% PEG (all w/w)

System	% NaCl					
	0	2	4	6	8	10
1	−2.45	−2.40	−2.21	−2.41	−2.50	−2.49
2	−2.42	−2.38	−2.42	−2.37	−2.43	−2.51
3	−2.34	−2.18	−2.30	−2.28	−2.22	−2.37

5.3. Partition coefficient fitting

A number of alternatives were searched for the expression of the partition coefficient (K_p) of the α-amylase and of the contaminant proteins from a *B. subtilis* supernatant. The sigmoidal Boltzman (Eq. 13) used to express the α-amylase data gave a very good fit to the experimental values as illustrated in Fig. 5. Some of the discrepancy seen at the very low values of Log K_p can be attributed to the error associated with the measurement of very low protein

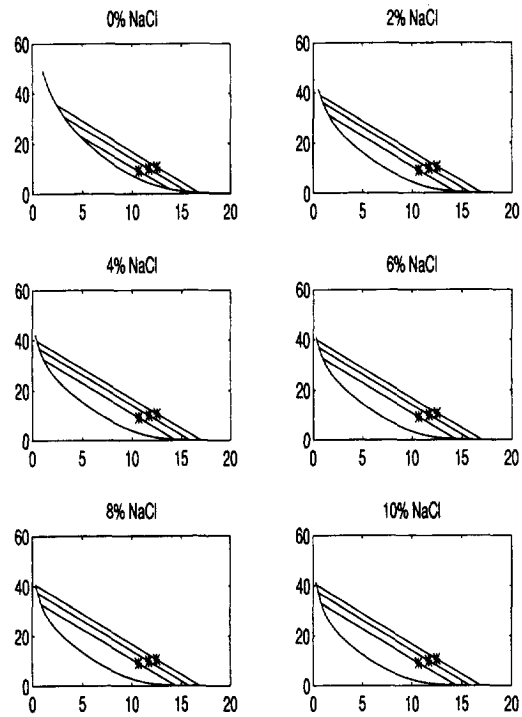

Fig. 4. Tie line gradient and binodial location variations at different NaCl concentrations.

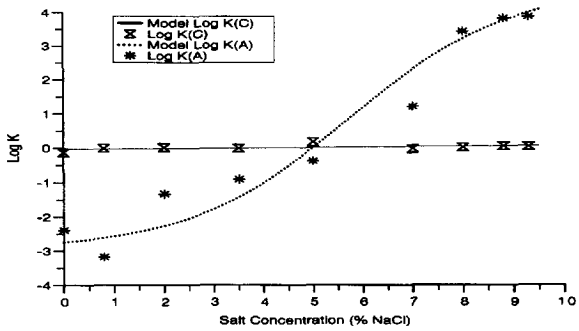

Fig. 5. Comparison of α-amylase (A) and contaminant (C) data and model fit.

concentrations ($K=10^{-2}$–10^{-3}). Protein contaminants were fitted by a straight line (Eq. 14).

One of the main problems encountered in the modelling was that the equation system was non-linear due to the phase equilibrium behavior and to the presence of a recycle. This meant that a powerful and robust equation based simulator was required to handle the simulation. The software chosen (SPEEDUP) can readily be used for steady state and dynamic simulation so it seemed ideal for the task. SPEEDUP can also process experimental data to estimate the coefficients of a given general equation to the data and this proved very useful during the model design stage.

5.4. Sample examples

The complete model has been successfully used to study two very different cases.

5.4.1. Small PEG phase

Running the model with large bottom phases and smaller top phases in both stages (Fig. 6) allows for the NaCl to be significantly reduced (diluted) when the PEG is transferred into the second stage. A large fresh phosphate phase (F_5) is added as shown in Fig. 2 thus obtaining dramatically different partition coefficients for the product protein in Stage 1 (K_1) and stage 2 (K_3) as shown in Fig. 5 and Fig. 7. The overall system diagram of material balances is shown in Fig. 8. M_1 and M_2 represent the overall composition of Stage 1 and 2. The two binodials shown correspond to the NaCl concentrations of the stages (8.8% and 2.0% respectively). Such a system dia-

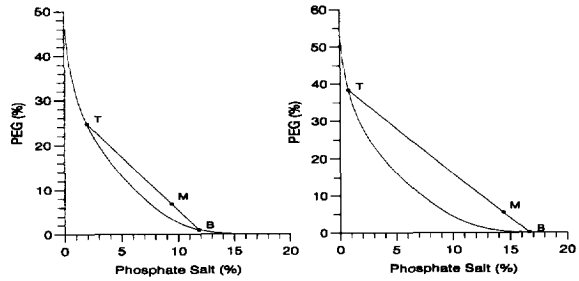

Fig. 6. Effect of large bottom phases on the equilibrium and phase separation in Stage 1 and Stage 2.

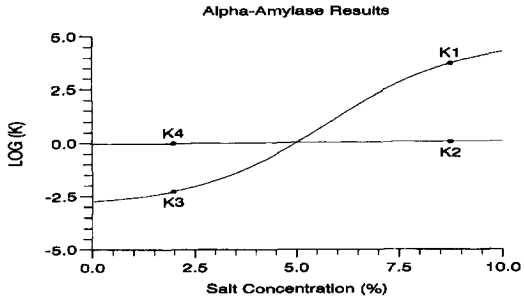

Fig. 7. Partition coefficients for system with small PEG and large phosphate phases thus allowing for important NaCl dilution between Stage 1 (K_1,K_2) and Stage 2 (K_3,K_4).

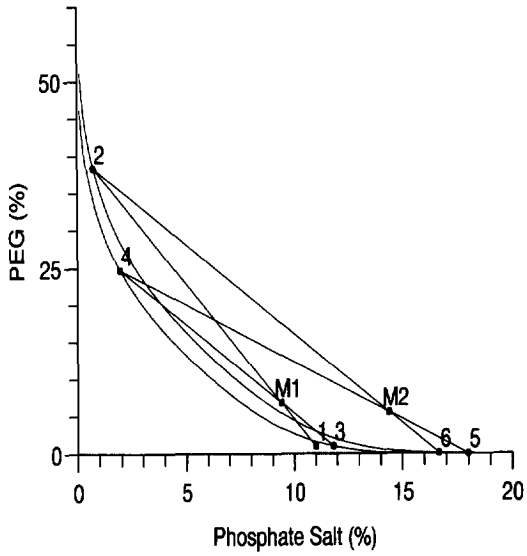

Fig. 8. Overall system diagram for system with large bottom phases. M_1 and M_2 represent overall compositions of Stage 1 and 2. Numbers refer to feeds in Fig. 2. The two binodials correspond to NaCl concentrations of 8.8% and 2.0%, respectively.

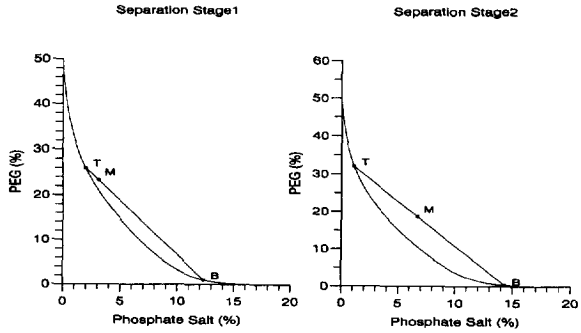

Fig. 9. Effect of large top phases on the equilibrium and phase separation in Stage 1 and Stage 2.

gram of material balances is a very clear representation of an extraction and back-extraction system. A purification factor of 3.94 is obtained for the protein product (α-amylase) in this system. This seems to be the first time such a diagram is used to represent extraction and back-extraction in aqueous two-phase systems.

5.4.2. Large PEG phase

Running the model with large top phases in both stages (Fig. 9) only gives a relatively small dilution of the NaCl between stages (e.g. 5.9% and 4.3% respectively) thus resulting in a much smaller change in the partition coefficients between Stage 1 and 2 (K_1 and K_3 in Fig. 10). The overall system diagram of material balances is shown in Fig. 11. Here, with the smaller dilution of the NaCl, the binodials are much closer together and a smaller purification factor for the protein product of 2.09 is obtained when compared to the case with a small PEG phase.

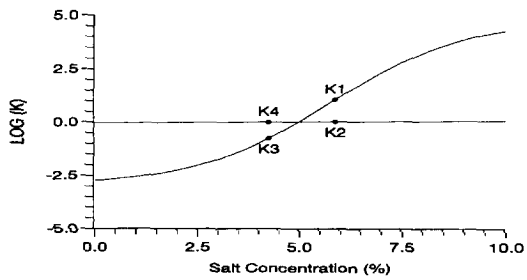

Fig. 10. Partition coefficients for system with large PEG phases allowing for small dilution between Stage 1 (K_1,K_2) and Stage 2 (K_3,K_4).

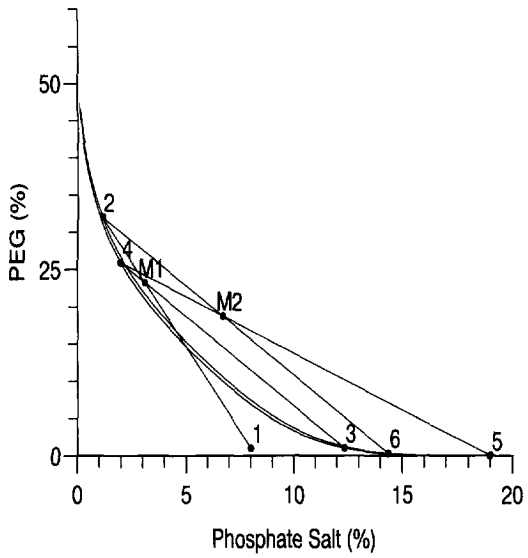

Fig. 11. Overall system diagram for system with large top phases. M_1 and M_2 represent overall compositions of Stage 1 and 2. Numbers refer to feeds in Fig. 2. The two binodials correspond to NaCl concentrations of 5.9% and 4.3%, respectively.

5.5. Kinetics of phase separation

5.5.1. Mixing

Data is already available for the constant I from Eq. (16) and so the time required for macromixing can be found for a range of different impeller types [10]. However as already stated, in aqueous two-phase systems mixing is easily achieved [9].

5.5.2. Phase separation

In a batch separator the height of the interphase changes as a function of time until the system is fully settled. This has been recently investigated in some detail [9]. However, no correlations to describe this phenomena have yet been developed. Settling can also be carried out continuously in a simple square decanter. A rectangular unit of 1-l volume, 4 cm wide, 5 cm in height and 50 cm long was recently designed and used [11] and the residence time needed for total separation of the phases was very similar to the settling time needed in a batch separator of a similar height (e.g. 6–7 min for a PEG4000–phosphate system with a stability ratio of 0.18).

An adequate expression needs to be used to find

the settling rate (height of the interphase as a function of time) and thus the time necessary for the two phases to separate. A correlation, that describes the functionality given by Eqs. (18,19) that was used by Golob and Modic [12] for aqueous–organic two phases, is presently being investigated and used with aqueous systems and is given by:

$$\frac{dh}{dt}\frac{\mu_c}{\sigma} = \text{const.}\left(\frac{\mu_d}{\mu_c}\right)^a\left(\frac{\sigma_w}{\sigma}\right)^b\left(\frac{\Delta\rho}{\rho_c}\right)^c \qquad (22)$$

where μ_c = viscosity of the continuous phase, μ_d = viscosity of the dispersed phase, σ = surface tension between the two phases, σ_w = surface tension of water at 20°C, ρ_c = density of the continuous phase and a,b,c = constants.

The question of which phase is the continuous one in an aqueous two-phase system is thus extremely important and has been recently addressed [9]. Fig. 12 shows the binodial for a PEG4000–phosphate system with tie-lines that represent the systems studied. Marked on each tie-line is the point of transition where the continuous phase changes (phase inversion point). Generally, moving away from this point along either side of the tie-line, phase separation times will increase. This can be seen in Fig. 13. The phase inversion point which, in this case, is represented by the vertical line (Fig. 12) occurs at a phosphate concentration which corresponds to that of the critical point. The phase inversion line should pass through the critical point.

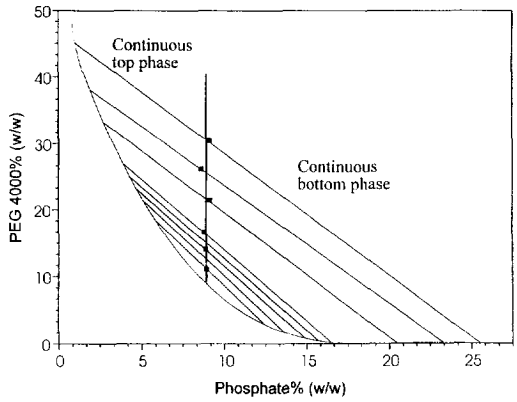

Fig. 12. Phase diagram for PEG4000/phosphate at pH 7, phase inversion point, ■. To the left of vertical line, systems have a continuous top phase and to the right a continuous bottom phase.

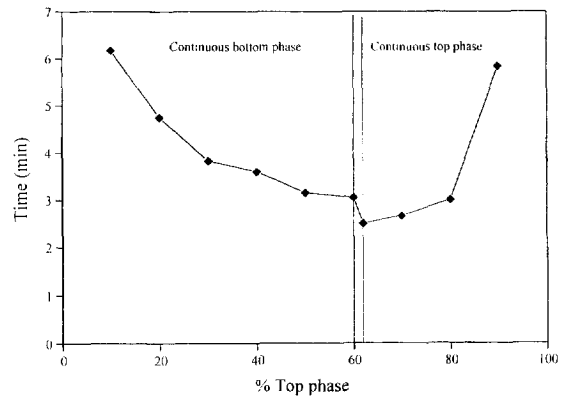

Fig. 13. Effect of the change in % top phase on phase separation time. PEG4000–phosphate systems on tie-line going through the point PEG (12.5%), phosphate (10.7%) with a stability ratio of 0.18.

To obtain a generalised description of the process of separation independently of the height of the initial dispersion, two variables have been defined-

$$h^* = \frac{h}{h_o} \qquad (23)$$

$$t^* = \frac{t}{h_o} \qquad (24)$$

where h is the height of the dispersion or interphase, h_o is the total height of dispersion which is equal to the height of the ATPS, h^* the relative height of the dispersion and t^* the normalised separation time which has units of 1/velocity. Also, an average separation rate has been defined as the ratio of the initial height and the time required for complete separation, t_s:

$$V_s = \frac{h_o}{t_s} \qquad (25)$$

The time for phase separation has been studied at small scale (5-g systems) and large scale (1300-g systems) for five systems with stability ratios of 0.038, 0.09, 0.12, 0.15 and 0.18. Fig. 14a shows the relative height of dispersed phase as a function of the normalised separation time for different values of the stability ratio. The settling profiles were very similar for the 5-g and 1300-g systems. The normalised separation time is shown to be independent of the height of the dispersed phase for systems with

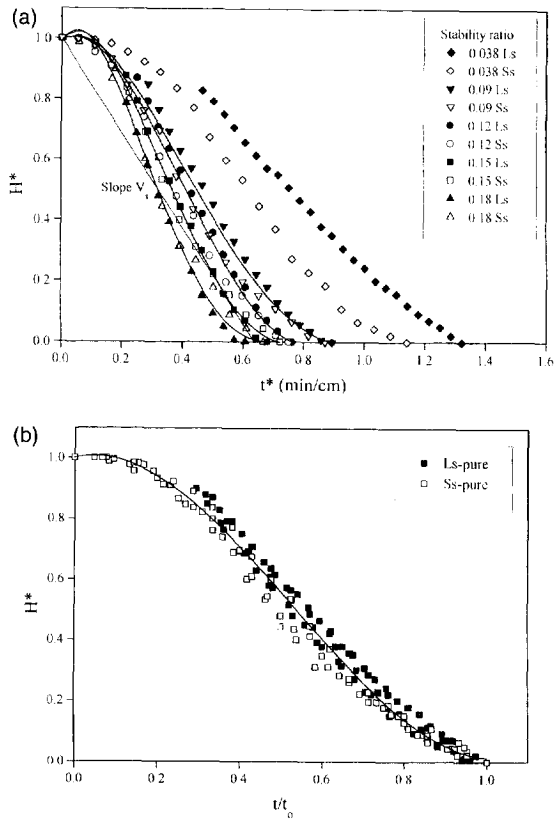

Fig. 14. Change in the normalised separation time ($t^* = t/h_o$) (a) and relative separation time (t/t_s) (b), with relative height of dispersion ($h^* = h/h_o$) as a function of the stability ratio for 5-g systems (Ss = small scale; open symbols) and for 1300-g systems (Ls = large scale; closed symbols).

stability ratios between 0.09 and 0.18. At a stability ratio of 0.038 though, phase separation times are clearly different. Fig. 14a also shows a straight line of slope V_s, for the curve of stability ratio 0.18, which corresponds to Eq. (25). Given the shape of the settling curve, V_s can also be found from the settling time when $h^* = 0.5$. When NaCl was added at high concentrations to the systems (e.g. 8.8%) as it is sometimes done to manipulate partition coefficients (Fig. 5) the settling profiles were very similar but there was a marked decrease in phase separation time [9].

If, instead of plotting h^* vs. t^* we plot h^* vs. t/t_s then all the points fall virtually on the same line (Fig. 14b). This means that the actual mechanism of phase separation is the same in all systems. In aqueous–organic systems when the rate of sedimentation is greater that the rate of coalescence, then a sigmoidal curve like that shown in Fig. 14b is observed (rate of coalescence is the limiting step). If the rate of sedimentation is the limiting step, then an exponential curve is observed.

Measurements of the density and viscosity of the top and bottom phases have been carried out [9] and the surface tension between the phases is presently being evaluated. This will allow the determination of appropriate constants in Eq. (22) and find values for the settling velocity and settling time whether we are in the regime to the left or right of the phase inversion line in Fig. 12. In addition, an evaluation of droplet diameter d_d is being carried out as this will, to some extent, be determined by t_m (Eq. 19) and will, at least indirectly, have an effect on dh/dt and t_s although it does not appear explicitly in Eq. (22). Preliminary evaluation of droplet diameter can be done from photographs taken during settling of a system with a continuous top phase and one with a continuous bottom phase. Also, d_d varies with time as coalescence is the limiting rate and smaller droplets that coalesce will give rise to larger ones. Two such photographs are shown in Fig. 15.

Fig. 15 shows two pairs of PEG4000–phosphate systems. Each pair lies on the same tie-line but they have different volume ratios so they are on different sides of the phase inversion line (Fig. 12). The systems shown in Fig. 15a are on the tie-line that goes through the point with a stability ratio of 0.18, which is relatively near the binodial curve. The systems shown in Fig. 15b are on the tie-line that goes through the point with a stability ratio of 0.5, which is rather far from the binodial curve. Each system was vigorously shaken for 30 s and allowed to separate, photographs were taken at intervals during the separation, before mixing and at 15, 30, 45, 60, 75, 90, 105, and 120 s. Fig. 15 shows the photographs taken after 60 s. It could be clearly seen that the systems on the left of Fig. 15a and b have continuous top phases (where droplets fall and coalesce) and the systems on the right have continuous bottom phases (where droplets rise and coalesce). In Fig. 15a, the system on the left (continuous top phase) separates faster than the one on the right whereas in Fig. 15b, the one on the right (continuous bottom phase) separates faster than the one on the

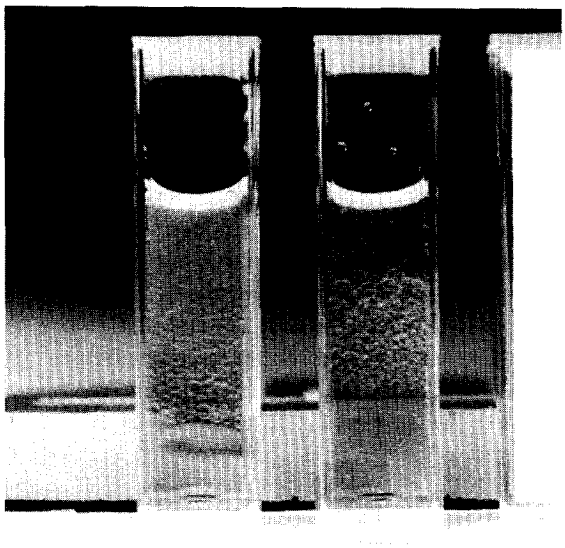

(a)

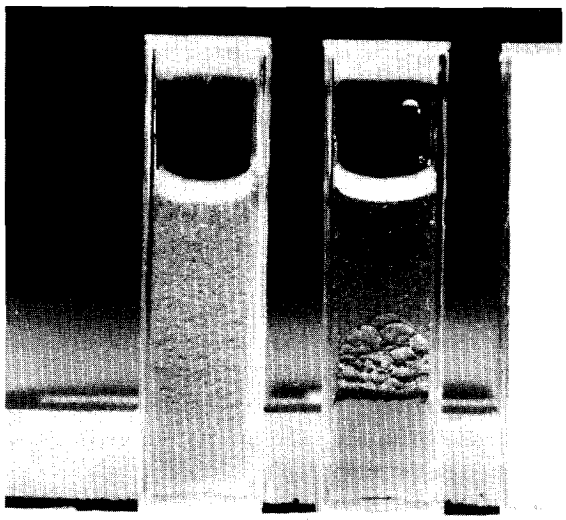

(b)

Fig. 15. PEG4000–phosphate systems with different stability ratios at 60 s after settling begins. In (a) and (b), the systems on the left have a continuous top phase and the ones on the right have a continuous bottom phase. Systems in (a) are on the same tie line which goes through the point with a stability ratio of 0.18 to the left and right of the phase inversion point. In (b), the systems have a stability ratio of 0.5, the rest is the same as in (a).

left. The observation made in Fig. 14, that the rate of coalescence controls the kinetics of phase separation seemed confirmed clearly from the analysis of the photographs. A comprehensive investigation aimed at a more fundamental understanding of the mechanisms and regimes controlling the kinetics of gravitational ATPS separation is presently being carried out. The effect of mixing on drop size and coalescence is also being studied.

6. Conclusions

An extended mathematical model that describes the continuous, steady state operation of an aqueous two-phase system for protein extraction based on steady state mass balances is presented in this paper. The main conclusions of the investigation and simulation carried out with this model follow.

Phase equilibrium is described by a binodial curve and the appropriate tie-lines under specific NaCl concentrations. The phase equilibrium is fitted by an empirical equation that relates PEG to the phosphate and NaCl concentration. Tie lines are fitted to a straight line equation of constant slope, $D_1 = -2.4$, which is valid over the whole range of NaCl concentrations.

The partition coefficient for the α-amylase data as a function of the added salt (NaCl) is fitted to a sigmoidal Boltzman curve and gives a very good fit. High partition coefficients can be achieved for the α-amylase at high NaCl concentrations and back partitioning is possible due to the very low partition in low NaCl concentrations. Contaminant protein data is fitted by a straight line and the partition coefficient is fairly close to 1 over the NaCl range.

Two simulations were carried out to show the effect of phase ratio on the system. Working with a large salt phase gave very good purification due to the drastic dilution of the NaCl between stages which aided the forward extraction. In the second case, the large PEG phase led to reduced dilution of the NaCl giving much poorer purification in the forward and back extractions.

The model has also been extended to account for phase separation kinetics and thus aspects of continuous processing. The present work in modelling the rate of settling of the two phases (and thus the time for complete separation) using appropriate correlations has been presented and discussed in some detail.

References

[1] P.A. Albertsson, Partition of Cell Particles and Macromolecules. Wiley, New York, 1986, 3rd ed.
[2] H. Hustedt, Biotechnol. Lett., 8 (1986) 791–796.
[3] M.R. Kula, K.H. Kroner and H. Hustedt, Adv. Biochem. Eng., 24 (1982) 73–118.
[4] O. Cascone, B.A. Andrews and J.A. Asenjo, Enzyme Microb. Technol., 13 (1994) 629–635.
[5] C. Hodgson, Partition and Purification of tPA in Aqueous Two-Phase Systems, Ph.D. thesis, The University of Reading, 1992.
[6] A.S. Schmidt, A.M. Ventom and J.A. Asenjo, Enzyme Microb. Technol., 16 (1994) 131–142.
[7] S.L. Mistry, J.A. Asenjo and C.A. Zaror, Bioseparation, 3 (1993) 343–358.
[8] S.L. Mistry, J.C. Merchuk and J.A. Asenjo, Mathematical Modelling and Computer Simulation of Continuous Aqueous Two-Phase Protein Extraction, in D.L. Pyle (Editor), Separations for Biotechnology 3, The Royal Society of Chemistry, 1994, 321–328.
[9] A. Kaul, R. Pereira, J.A. Asenjo and J.C. Merchuk, Biotechnol. Bioeng., 48 (1995) 246–256.
[10] A. Pandit, C. Rielly, K. Niranjan and J. Davidson, Chem. Eng. Sci., 44 (1989) 2463–2474.
[11] R.A.M. Pereira, Phase Separation Studies for Polyethylene Glycol–Phosphate Two-Phase Systems, B.Sc. dissertation, The University of Reading, 1994.
[12] J. Golob and R. Modic, Trans. IChemE, 55 (1977) 207–211.